Version of Record: https://www.sciencedirect.com/science/article/pii/S2451910321000417
Manuscript_8a8301a4085aca6e007868f2b549e0c3

Review Article

Light-addressable potentiometric sensors (LAPS) for cell monitoring and biosensing

Tatsuo Yoshinobu[1], Michael J. Schöning[2,3]

Addresses

[1] Graduate School of Biomedical Engineering, Tohoku University, Aza-Aoba 6-6-05, Aramaki, Aoba-ku, Sendai 980-8579, Japan

[2] Institute of Nano- and Biotechnologies (INB), FH Aachen, Campus Jülich, 52428 Jülich, Germany

[3] Institute of Biological Information Processing (IBI-3), Research Centre Jülich, 52425 Jülich, Germany

Corresponding authors: Tatsuo Yoshinobu (nov@tohoku.ac.jp);
Michael J. Schöning (schoening@fh-aachen.de)

Abstract

The light-addressable potentiometric sensor (LAPS) represents a versatile platform for chemical and biosensing. Thanks to the light-addressability, the flat sensor surface of a LAPS can be flexibly divided into areas or pixels, each functioning as an independent sensor that can be modified with various sensing materials for measuring different ions or molecules. Since it first appeared in the late 1980s, it has been applied to various cells and biological samples, driven by technological developments. In this short review, the principles of a LAPS and its variants are briefly described focusing on recent trends and applications to cells and biosensing.

Keywords

Light-addressable potentiometric sensor (LAPS), cell monitoring, biosensing, amplitude-mode LAPS, phase-mode LAPS, scanning photo-induced impedance microscopy (SPIM)

Highlights

- LAPS enables spatially resolved detection of ions or molecules
- It has a high flexibility of setup to be applied to cells and biological samples
- For LAPS, various biosensing principles can be adopted to detect biomolecules
- Applications are analysis of cellular metabolism, neural activity, DNA hybridization

1. Introduction

A light-addressable potentiometric sensor (LAPS) [1-3] is a semiconductor-based sensing platform for measuring ions and molecules in a spatially-resolved manner. It has a layer structure identical to that of the gate region of an ion-sensitive field-effect transistor (ISFET) [4], in which the Nernst potential on the gate surface controls the charge carriers in the semiconductor device. Thanks to this structural similarity, many of the technologies developed for ISFETs are transferable to a LAPS. In addition, the light-addressability of a LAPS makes it possible to use a light beam to define arbitrary shapes and sizes of measured areas at particular positions on the sensor surface. It is therefore natural that researchers focused, even in the earliest publications [1,5], on the application of LAPS for studying the metabolic activity of cells. Within the last two decades their usage found extension for analytical purposes such as recording of different types of bacteria, yeast and other cells, detection of DNA, heavy metal ions and proteins. In this short review, the principle of a LAPS and its applications to cells and biosensing in recent years will be summarized.

2. Principles and operation modes

2.1. Setup of a LAPS

Figure 1a shows a typical setup for LAPS measurement. The sensor plate consists of a semiconductor substrate covered with an insulating layer on top and an ohmic contact on the rear surface. The surface of the insulating layer is in contact with the analyte solution to be measured, and a Nernstian potential ϕ, which is dependent on the activity of the analyte, is built up at the electrolyte – insulator interface. This electrolyte – insulator – semiconductor (EIS) system is externally biased, so that a depletion layer is formed at the insulator – semiconductor interface. Usually, the sensor plate is virtually grounded via a transimpedance amplifier (TIA), which operates as an ammeter, and a DC (direct current) voltage V_{bias} is applied to the reference electrode (RE), or in other words, the sensor plate is biased to $-V_{\mathrm{bias}}$ with respect to the RE. Here, the effective voltage applied to the EIS system is the sum of V_{bias} and ϕ, and the depletion layer grows as the EIS system is more reverse-biased until inversion occurs. The variation of the thickness of the depletion layer is detected in the form of an alternating current (AC) signal, which is generated by illumination and correlated with the activity of the target analyte.

2.2. Generation of signals

Figure 1b shows energy band diagrams illustrating the generation of the AC current

signal by modulated illumination. When the light is turned on, electron – hole pairs are generated inside the semiconductor and diffuse toward the depletion layer. Electrons and holes are separated by the electric field inside the depletion layer, resulting in a transient current. When the light is turned off, excess holes inside the depletion layer are removed by recombination, resulting in a transient current in the reverse direction [2,3].

The repeated generation of alternating currents by modulated illumination can be represented by an AC current source I_{photo} in the circuit model of a LAPS shown in Figure 1c. The AC current I_{photo} is divided between the capacitance of the depletion layer C_{d} and the capacitance of the insulating layer C_{i} in the illuminated area, and the AC current that flows through the latter is externally measured as a LAPS signal I. The series impedance Z includes the impedance of the solution, the resistance of the semiconductor, the contact resistance, and the input impedance of the TIA. A part of the signal current is lost by capacitive coupling between the solution and the semiconductor substrate, which is represented as a return current that flows through the admittance Y of the non-illuminated area. If both Z and Y are negligibly small, the AC current signal I is given by a simple formula (see eq. 1),

$$I = I_{\mathrm{photo}} \times \frac{C_{\mathrm{i}}}{C_{\mathrm{i}}+C_{\mathrm{d}}} \ , \qquad (1)$$

which varies as illustrated in Figure 1d left, reflecting the variation of C_{d} as a function of V_{bias}.

2.3. Measurement modes

Figure 1d left shows the variation of I as a function of V_{bias}. As the EIS system is more reverse-biased, C_{d} becomes smaller and I becomes larger. When ϕ changes in response to the activity of the analyte (the figure shows the case of H^+ ions as an example), the current – voltage curve shifts along the voltage axis. In the amplitude mode of LAPS operation, this shift is correlated with the activity of the analyte. It should be noted that the method is intrinsically potentiometric since no DC current flows through the insulator [2,3].

Figure 1d middle shows the scanning photo-induced impedance microscopy (SPIM) mode operation, in which the variation of Z is detected [6-8]. This mode can be applied, for example, to monitor the change of the impedance of an object such as a cell, a cell layer, or a tissue directly cultured on the sensor surface.

Figure 1d right shows the principle of the phase-mode LAPS, in which the phase rather than the amplitude of the AC current signal I is measured to detect the variation of the angle of impedance inside the semiconductor. This mode is advantageous in

certain situations where the amplitude may fluctuate [3].

2.4. Light-addressability

Light-addressability is a unique feature of a LAPS, which allows a light beam to address a particular position of interest on the sensor surface to be investigated. It allows definition of a plurality of measurement sites that function as a set of independent sensors [1]. These sensors can be designed to investigate either a single species in a plurality of samples in isolated multi-wells or a plurality of species in a single sample, with individual measurement sites modified with different sensing materials in the latter case. Furthermore, a LAPS can serve also as a platform of chemical imaging by addressing a two-dimensional array of measurement sites, each corresponding to a pixel in a chemical image [9,10].

2.5. Related technologies

New technologies related to a LAPS have been developed to enhance its performance and broaden its field of application. As for the sensor materials, various insulators and semiconductors have been tested, including HfO_2 films for sensing NH_4^+ [11], silicon on sapphire functionalized with self-assembled organic monolayers for high sensitivity [12], ZnO nanorods for increased AC photocurrent and high resolution [13], InGaN for increased AC photocurrent [14] and indium gallium zinc oxide (IGZO) to avoid interference of the ambient light [15,16]. To achieve higher spatial resolutions, new methods for excitation of charge carriers have been also proposed. The use of the two-photon effect achieved a submicrometer resolution of 0.8 μm [8], and recently, the use of an electron beam instead of a light beam was proposed [17].

While the photocurrent in a LAPS is a signal to read out the change of the potential at the illuminated position on the surface, it can also play a role to deliver a faradaic current for an electrochemical reaction taking place at the illuminated position on the surface. Such techniques have been applied for stimulating neurons [18-21], ion sensing [22], detection of DNA hybridization [23,24] and mapping of cell surface charges [25]. They are termed as light-addressable electrode (LAE) [21,26], light-activated electrochemistry [22-24,27] or photoelectrochemical imaging [14,25], depending on their purposes.

A different approach of chemical imaging from that based on a LAPS is to utilize an array of discrete sensors: CMOS ion image sensors [28-30] and ISFET arrays [31,32] are advantageous for acquisition of chemical images with a large number of pixels at a high frame rate. In contrast to a device with hard-wired pixels, the pixel layout in a LAPS can be flexibly arranged at the time of use. Especially, when it comes to *in vivo*

measurement of cells, flexible addressing is an advantage as the position of a cell is generally unknown before their culturing.

3. LAPS for cell monitoring

Since its invention, analysis of cells has been considered as one of the main targets of a LAPS [1,33,34]. A LAPS can measure the acidification rate as an indicator of the metabolic activity of cells. Such a system is called a microphysiometer and was put into the market as a Cytosensor® [5,35]. Quantification of the metabolic activity is useful in pharmaceutical sciences, for example, to test the effect of a certain drug on cells or a cell culture, immobilized on the LAPS chip, in a drug screening process. The target cells of recent studies include various bacteria such as *Escherichia coli* [36-39], *Corynebacterium glutamicum* [38-40] and *Lactobacillus brevis* [38,39], breast cancer cells [41,42], hepatoma cells [43,44], Chinese hamster ovary cells [45] and macrophages [46]. For example, Figure 2a compares the acidification rates resulting from metabolism of three different bacteria [38]. In these studies, the light-addressability allowed integration of multiple measurement sites on a single sensor plate [38-40]. Combination of the LAPS with a microfluidic system enables both continuous drug delivery and exchange of nutrient solution [41,43,44]; in addition, integration of an on-chip cryopreservation system for enhanced cell recovery on the sensor chip was realized by electrospun nanofibers for fast thawing [45].

Another modality of assay is the one that relies on the potential change as a result of specific binding on the surface of a LAPS: Monoclonal antibodies [47] and aptamers [48] immobilized on a LAPS surface were employed as probes to capture and detect circulating tumor cells. Aptamers were also selected as bioreceptors to detect adenosine triphosphate (ATP) released by taste receptor cells [49,50]. Yet another approach is recording of extracellular potentials, which was reported for olfactory sensory neurons [51] and taste receptor cells [50] cultured on a LAPS surface. Figure 2b shows a schematic of such dual measurement of ATP release and extracellular potential of taste receptor cells [50].

The light-addressability also serves as a basis of cell imaging by using a scanning light beam. For example, a multilayer of yeast *Saccharomyces cerevisiae* was visualized by an inert LAPS without pH sensitivity [52], where the contrast was based on the surface negative charge and the local impedance of the cells. The surface charge of a single live cell was visualized under physiological conditions by a photoelectrochemical imaging system (PEIS) [25] using a setup similar to that of a LAPS but having an indium tin oxide (ITO) -coated glass substrate. Figure 2c depicts a further example, in

which an AC photocurrent image of a human osteosarcoma cell obtained with a LAPS structure of InGaN/GaN on sapphire is compared with its optical image [14].

In vivo analysis of the brain is another potential application of a LAPS. Figure 2d shows the concept of the multiplexed pH probe [53,54], which consists of a millimeter-sized LAPS attached at the tip of an optical fiber bundle. The probe can be implanted chronically into the brain (hippocampal formation of rats) for a spatially resolved measurement of local pH fluctuations, studying physiological and pathophysiological conditions.

4. Biosensing and application to biological samples

A LAPS and related technologies have also been employed as platforms of biosensing and they have been applied to different biological samples [55]. Biocatalysis and selective binding are the typical biosensing principles. In the former type, protons or other chemical species produced during enzymatic reaction are often detected. Figure 3a shows an example of glucose sensing with glucose oxidase; the sensor was further on adopted to real biological samples, like blood and urine [56]. Monitoring of systematic enzymatic degradation of a polymer film shown in Figure 3b is another example [13]. In the latter type, the probe molecules immobilized on the sensor surface capture target species in the specimen, or *vice versa*, and the change of the surface potential is detected.

Because of the potential importance in biomedical applications, detection of DNA and DNA-related processes are often the targets of LAPS-based biosensors; various combinations of probe and target species have been reported. For example, a positively charged polyelectrolyte layer of PAH (poly(allylamine hydrochloride)) on the sensor surface was used for electrostatic coupling and detection of double-stranded DNA (dsDNA) molecules, which are negatively charged [57]. Figure 3c demonstrates the quantification of single-stranded DNA (ssDNA) of *E. coli* O157:H7 cells based on the potential change by hybridization with complimentary ssDNA probes immobilized on the sensor surface [58]. Immunosensing is another strategy of biosensing. DNA methylation was quantified by measuring the potential change due to binding of 5-methylcytosine (5mC) sites of ssDNA and 5mC-antibody [59], where the target ssDNA was anchored on the sensor surface and the antibody was captured. Nucleic acids can also serve as sensing elements such as aptamers [60,61] and DNAzymes [60]. Figure 3d shows the quantification of Alpha-fetoprotein (AFP) by potential change due to the binding of AFP to aptamers anchored to gold nanoparticles on the sensor surface [61].

LAPS-based sensing systems are also applied to food analysis. Detection of *E. coli* in orange juice [37] and heavy metal ions in fish [62] and rice [63] are examples of such systems, which would be of practical use in ensuring the safety of foods.

5. Conclusions

The simple structure and the flexible layout / integration of various measurements on a single sensor plate are the main advantages of a LAPS. Virtually any process that affects the potential on the sensor surface can be target of a LAPS-based measurement. Monitoring of the metabolic activity of cells, recording of neural activities, measurement of specific biomolecules and detection of DNA hybridization with LAPS-based measurement systems have been reported (see Table 1) as well as non-biological applications in the fields of electrochemistry and materials science. Obviously, a good design of chemistry used for immobilization and specific binding of probe and target molecules is of essential importance to achieve a highly sensitive and selective measurement, together with the improvement of the sensor plate, measurement electronics and data processing. Imaging is one of the directions, into which future efforts should be directed to explore the further possibilities of LAPS-based analysis systems. Integration with microfluidics is another direction, which is indispensable for handling micro-volume samples in biomedical and pharmaceutical applications. Yet another possibility of a LAPS is that it can be combined with other light-addressing technologies such as LAE for stimulating, for example, the target cell to be measured by a LAPS. The next decade will see more sophisticated applications of LAPS-based systems for cells and biological samples, also emphasizing on single-cell recording.

Conflict of interest statement

The authors declare no conflict of interest.

Acknowledgements

This research did not receive any specific grant from funding agencies in the public, commercial, or non-for-profit sectors. The authors would like to thank H. Iken for technical assistance (adaptation of figures, table).

References

[1] D.G. Hafeman, J. Wallace Parce, H.M. McConnell, Light-addressable potentiometric sensor for biochemical systems, Science 240 (1988) 1182–1185. DOI: 10.1126/science.3375810

[2] T. Yoshinobu, K. Miyamoto, C.F. Werner, A. Poghossian, T. Wagner, M.J. Schöning, Light-addressable potentiometric sensors for quantitative spatial imaging of chemical species, Annu. Rev. Anal. Chem. 10 (2017) 225–246. DOI: 10.1146/annurev-anchem-061516-045158

[3] T. Yoshinobu, S. Krause, K. Miyamoto, C.F. Werner, A. Poghossian, T. Wagner, M.J. Schöning, (Bio-)chemical sensing and imaging by LAPS and SPIM, in: M.J. Schöning, A. Poghossian (Eds.) Label-Free Biosensing: Advanced Materials, Devices and Applications (Springer Series on Chemical Sensors and Biosensors), Springer, Berlin, Heidelberg, 2018, pp.103–132. DOI: 10.1007/5346_2017_22

[4] P. Bergveld, Development of an ion-sensitive solid-state device for neurophysiological measurements, IEEE Trans. Biomed. Eng. 17 (1970) 70–71. DOI: 10.1109/tbme.1970.4502688

[5] H.M. McConnell, J.C. Owicki, J. W. Parce, D.L. Miller, G.T. Baxter, H.G. Wada, S. Pitchford, The cytosensor microphysiometer: Biological applications of silicon technology, Science 257 (1992) 1906–1912. DOI: 10.1126/science.1329199

[6] S. Krause, H. Talabani, M. Xu, W. Moritz, J. Griffiths, Scanning photo-induced impedance microscopy – an impedance based imaging technique, Electrochim. Acta 47 (2002) 2143–2148. DOI: 10.1016/S0013-4686(02)00088-9

[7] F. Wu, I. Campos, D.-W. Zhang, S. Krause, Biological imaging using light-addressable potentiometric sensors and scanning photo-induced impedance microscopy, Proc. R. Soc. A 473 (2017) art. no. 20170130. DOI: 10.1098/rspa.2017.0130

[8] L. Chen, Y. L. Zhou, S. H. Jian, J. Kunze, P. Schmuki, S. Krause, High resolution LAPS and SPIM, Electrochem. Commun. 12 (2010) 758–760. DOI: 10.1016/j.elecom.2010.03.026

[9] M. Nakao, T. Yoshinobu, H. Iwasaki, Scanning-laser-beam semiconductor pH-imaging sensor, Sens. Actuators B 20 (1994) 119–123. DOI: 10.1016/0925-4005(93)01199-E

[10] T. Liang, Y. Qiu, Y. Gan, J. Sun, S. Zhou, H. Wan, P. Wang, Recent developments of high-resolution chemical imaging systems based on light-addressable potentiometric sensors (LAPSs), Sensors 19 (2019) art. no. 4294. DOI:

10.3390/s19194294

[11] J. Yang, T. Lu, J. Wang, C. Yang, D.G. Pijanowska, C. Chin, C. Lue, C. Lai, LAPS with nanoscaled and highly polarized HfO_2 by CF_4 plasma for NH_4^+ detection, Sens Actuators B 180 (2013) 71 – 76. DOI: 10.1016/j.snb.2012.03.025

[12] J. Wang, Y. Zhou, M. Watkinson, J. Gautrot, S. Krause, High-sensitivity light-addressable potentiometric sensors using silicon on sapphire functionalized with self-assembled organic monolayers, Sens. Actuators B 209 (2015) 230–236. DOI: 10.1016/j.snb.2014.11.071

[13] Y. Tu, N. Ahmad, J. Briscoe, D.-W. Zhang, S. Krause, Light-addressable potentiometric sensors using ZnO nanorods as the sensor substrate for bioanalytical applications, Anal. Chem. 90 (2018) 8708–8715. DOI: 10.1021/acs.analchem.8b02244

[14] B. Zhou, A. Das, M.J. Kappers, R.A. Oliver, C.J. Humphreys, S. Krause, InGaN as a substrate for AC photoelectrochemical imaging, Sensors 19 (2019) art. no. 4386. DOI: 10.3390/s19204386

[15] C.-H. Chen, C.-M. Yang, A IGZO-based light-addressable potentiometric sensor on a PET substrate, Proc. FLEPS 2019 - IEEE Int. Conf. Flexible and Printable Sensors and Systems, 2019, art. no. 8792303. DOI: 10.1109/FLEPS.2019.8792303

[16] C.-M. Yang, C.-H. Chen, N. Akuli, T.-H. Yen, C.-S. Lai, Chemical illumination modification from an LED to a laser to improve the spatial resolution of IGZO thin film light-addressable potentiometric sensors in pH detections, Sens. Actuators (2020) art. no. 128953. DOI: 10.1016/j.snb.2020.128953

[17] W. Inami, K. Nii, S. Shibano, H. Tomita, Y. Kawata, Improvement of the spatial resolution of ion imaging system using thinned sensor substrate, Proc. SPIE 11521 (2020) art. no. 115210L. DOI: 10.1117/12.2573300

[18] H. Sugihara, M. Taketani, A. Kamei, H. Iwasaki, Two-dimensional sensor for measuring nerve cell activity and measurement device using it, Japanese Patent Disclosure, H09-005295, 1997.

[19] M.A. Colicos, B.E. Collins, M.J. Sailor, Y. Goda, Remodeling of synaptic actin induced by photoconductive stimulation, Cell 107 (2001), 605–616. DOI: 10.1016/S0092-8674(01)00579-7

[20] J. Campbell, D. Singh, G. Hollett, S.M. Dravid, M.J. Sailor, J. Arikkath, Spatially selective photoconductive stimulation of live neurons, Front. Cell. Neurosci. 8 (2014) 1–9. DOI: 10.3389/fncel.2014.00142

[21] J. Suzurikawa, M. Nakao, Y. Jimbo, R. Kanzaki, H. Takahashi, A light addressable

electrode with a TiO_2 nanocrystalline film for localized electrical stimulation of cultured neurons, Sens. Actuators B 192 (2014) 393–398. DOI: 10.1016/j.snb.2013.10.139

[22] Y. Yang, M. Cuartero, V.R. Gonçales, J.J. Gooding, E. Bakker, **Light-addressable ion sensing for real-time monitoring of extracellular potassium**, Angew. Chem. 57 (2018) 16801–16805. DOI: 10.1002/ange.201811268
The release of potassium ions from a single or a few cells was detected with a localized faradaic current in light-activated electrochemistry. The approach shows an example for dynamic electrochemistry studies.

[23] L. Zarei, R. Tavallaie, M.H. Choudhury, S.G. Parker, P. Bakthavathsalam, S. Ciampi, V.R. Gonçales, J.J. Gooding, DNA-hybridization detection on Si(100) surfaces using light-activated electrochemistry: A comparative study between bovine serum albumin and hexaethylene glycol as antifouling layers, Langmuir 34 (2018) 14817–14824. DOI: 10.1021/acs.langmuir.8b02222

[24] J. Wang, Z. Yang, W. Chen, L. Du, B. Jiao, S. Krause, P. Wang, Q. Wei, D.-W. Zhang, C. Wu, Modulated light-activated electrochemistry at silicon functionalized with metal-organic frameworks towards addressable DNA chips, Biosens. Bioelectron. 146 (2019) art. no. 111750. DOI: 10.1016/j.bios.2019.111750

[25] F. Wu, B. Zhou, J. Wang, M. Zhong, A. Das, M. Watkinson, K. Hing, D.-W. Zhang, S. Krause, Photoelectrochemical imaging system for the mapping of cell surface charges, Anal. Chem. 91 (2019) 5896–5903. DOI: 10.1021/acs.analchem.9b00304

[26] R. Welden, M.J. Schöning, P.H. Wagner, T. Wagner, Light-addressable electrodes for dynamic and flexible addressing of biological systems and electrochemical reactions, Sensors 20 (2020) art. no. 1680. DOI: 10.3390/s20061680

[27] S. Gautam, V.R. Gonçales, R.N.P. Colombo, W. Tang, S.I. Córdoba de Torresi, P.J. Reece, R.D. Tilley, J.J. Gooding, High-resolution light-activated electrochemistry on amorphous silicon-based photoelectrodes, Chem. Commun. 56 (2020) 7435–7438. DOI: 10.1039/d0cc02959a

[28] K. Sawada, T. Hattori, Ion image sensors and their application for visualization of neural activity, Jpn. J. Appl. Phys. 57 (2018) art. no. 1002A2. DOI: 10.7567/jjap.57.1002a2

[29] Y. Ogaeri, C. Kawakami, T. Hizawa, E. Shigetomi, Y. Shinozaki, T. Iwata, T. Noda, K. Takahashi, S. Koizumi, K. Sawada, Hydrogen ion image sensor with barrel array diffusion suppressor and hippocampal slice imaging, in:

TRANSDUCERS 2019 and EUROSENSORS XXXIII, 2019, art. no. 8808731, pp. 330–333. DOI: 10.1109/transducers.2019.8808731

[30] H. Horiuchi, M. Agetsuma, J. Ishida, Y. Nakamura, D. Lawrence Cheung, S. Nanasaki, Y. Kimura, T. Iwata, K. Takahashi, K. Sawada, J. Nabekura, **CMOS-based bio-image sensor spatially resolves neural activity-dependent proton dynamics in the living brain**, Nat. Commun. 11 (2020) art. no. 712. DOI: 10.1038/s41467-020-14571-y

A CMOS-based proton image sensor was employed to study the proton changes in the visual cortex induced by visual stimulation. The image sensor offers a high spatiotemporal resolution *in vivo*.

[31] J. Zeng, L. Kuang, N. Miscourides, P. Georgiou, A 128×128 current-mode ultra-high frame rate ISFET array with in-pixel calibration for real-time ion imaging, IEEE Trans. Biomed. Circuits Sys. 14 (2020) 359–372. DOI: 10.1109/tbcas.2020.2973508

[32] S. Honda, M. Shiomi, T. Yamaguchi, Y. Fujita, T. Arie, S. Akita, K. Takei, Detachable flexible ISFET-based pH sensor array with a flexible connector, Adv. Electron. Mater. 6 (2020) art. no. 2000583. DOI: 10.1002/aelm.202000583

[33] A. Poghossian, S. Ingebrandt, A. Offenhäusser, M.J. Schöning, Field-effect devices for detecting cellular signals, Seminars in Cell & Developmental Biology, 20 (2009) 41–48. DOI: 10.1016/j.semcdb.2009.01.014

[34] H. Yu, Q. Liu, P. Wang, Light addressable potentiometric sensor (LAPS) as cell-based biosensors, in: P. Wang, Q. Liu (Eds.), Cell-based Biosensors: Principles and Applications, Artech House, Norwood, MA, 2010, pp. 119–149.

[35] F. Hafner, Cytosensor® microphysiometer: Technology and recent applications, Biosens. Bioelectron. 15 (2000) 149–158. DOI: 10.1016/S0956-5663(00)00069-5

[36] P.M. Shaibani, K. Jiang, G. Haghighat, M. Hassanpourfard, H. Etayash, S. Naicker, T. Thundat, The detection of *Escherichia coli* (*E. coli*) with the pH sensitive hydrogel nanofiber-light addressable potentiometric sensor (NF-LAPS) Sens. Actuators B 226 (2016) 176–183. DOI: 10.1016/j.snb.2015.11.135

[37] P.M. Shaibani, H. Etayash, K. Jiang, A. Sohrabi, M. Hassanpourfard, S. Naicker, M. Sadrzadeh, T. Thundat, **Portable nanofiber-light addressable potentiometric sensor for rapid *Escherichia coli* detection in orange juice**, ACS Sens. 3 (2018) 815–822. DOI: 10.1021/acssensors.8b00063

A LAPS with a pH-sensitive hydrogel nanofiber was employed to detect acidification by metabolic activity of *Escherichia coli* in orange juice. Contamination of infected food with bacterial strains can be controlled.

[38] S. Dantism, D. Röhlen, T. Wagner, P. Wagner, M.J. Schöning, A LAPS-based differential sensor for parallelized metabolism monitoring of various bacteria, Sensors 19 (2019) art. no. 4692. DOI: 10.3390/s19214692

[39] S. Dantism, D. Röhlen, M. Dahmen, T. Wagner, P. Wagner, M.J. Schöning, **LAPS-based monitoring of metabolic responses of bacterial cultures in a paper fermentation broth**, Sens. Actuators B 320 (2020) art. no. 128232. DOI: 10.1016/j.snb.2020.128232

A LAPS system, loaded with three different model microorganisms, was applied to study the status of a paper-fermentation process, where the bioreactor serves as an alternative renewable energy source.

[40] S. Dantism, D. Röhlen, T. Selmer, T. Wagner, P. Wagner, M.J. Schöning, Quantitative differential monitoring of the metabolic activity of *Corynebacterium glutamicum* cultures utilizing a light-addressable potentiometric sensor system, Biosens. Bioelectron. 139 (2019) art. no. 111332. DOI: 10.1016/j.bios.2019.111332

[41] N. Hu, C. Wu, D. Ha, T. Wang, Q. Liu, P. Wang, A novel microphysiometer based on high sensitivity LAPS and microfluidic system for cellular metabolism study and rapid drug screening, Biosens. Bioelectron. 40 (2013) 167–173. DOI: 10.1016/j.bios.2012.07.010

[42] P.M. Shaibani, H. Etayash, S. Naicker, K. Kaur, T. Thundat, Metabolic study of cancer cells using a pH sensitive hydrogel nanofiber light addressable potentiometric sensor, ACS Sens. 2 (2017) 151–156. DOI: 10.1021/acssensors.6b00632

[43] T. Liang, C. Gu, Y. Gan, Q. Wu, C. He, J. Tu, Y. Pan, Y. Qiu, L. Kong, H. Wan, P. Wang, Microfluidic chip system integrated with light addressable potentiometric sensor (LAPS) for real-time extracellular acidification detection, Sens. Actuators B 301 (2019) art. no. 127004. DOI: 10.1016/j.snb.2019.127004

[44] T. Liang, Q. Wu, C. Gu, Y. Gan, J. Tu, Q. Hu, H. Wan, P. Wang, Light addressable potentiometric sensor (LAPS) integrated microfluidic system for real-time cell acidification detection, Proc. ISOEN 2019 - 18th International Symposium on Olfaction and Electronic Nose, 2019, art. no. 8823216. DOI: 10.1109/ISOEN.2019.8823216

[45] D. Özsoylu, T. Isık, Mustafa M. Demir, M.J. Schöning, T. Wagner, **Cryopreservation of a cell-based biosensor chip modified with elastic polymer fibers enabling ready-to-use on-site applications**, Biosens. Bioelectron (2021) art. no. 112983. DOI: 10.1016/j.bios.2021.112983

A LAPS sensor surface was modified with elastic electrospun fibers to prevent cryo-injury of cells cultured and preserved by freezing on chip. The modified sensor is integrated into a microfluidic system, enabling on-demand use after thawing.

[46] T. Wagner, W. Vornholt, C.F. Werner, T. Yoshinobu, K.-I. Miyamoto, M. Keusgen, M.J. Schöning, Light-addressable potentiometric sensor (LAPS) combined with magnetic beads for pharmaceutical screening, Phys. Medicine 1 (2016) 2–7. DOI: 10.1016/j.phmed.2016.03.001

[47] Y. Gu, C. Ju, Y. Li, Z. Shang, Y. Wu, Y. Jia, Y. Niu, Detection of circulating tumor cells in prostate cancer based on carboxylated graphene oxide modified light addressable potentiometric sensor, Biosens. Bioelectron. 66 (2015) 24–31. DOI: 10.1016/j.bios.2014.10.070

[48] F. Li, S. Hu, R. Zhang, Y. Gu, Y. Li, Y. Jia, Porous graphene oxide enhanced aptamer specific circulating-tumor-cell sensing interface on light addressable potentiometric sensor: Clinical application and simulation, ACS Appl. Mater. Interfaces 11 (2019) 8704–8709. DOI: 10.1021/acsami.8b21101

[49] C. Wu, L. Du, L. Zou, L. Zhao, P. Wang, An ATP sensitive light addressable biosensor for extracellular monitoring of single taste receptor cell, Biomed. Microdevices 14 (2012) 1047–1053. DOI: 10.1007/s10544-012-9702-3

[50] L. Du, J. Wang, W. Chen, L. Zhao, C. Wu, P. Wang, Dual functional extracellular recording using a light-addressable potentiometric sensor for bitter signal transduction, Anal. Chim. Acta 1022 (2018) 106–112. DOI: 10.1016/j.aca.2018.03.012

[51] L. Du, C. Wu, H. Peng, L. Zhao, L. Huang, P. Wang, Bioengineered olfactory sensory neuron-based biosensor for specific odorant detection, Biosens. Bioelectron. 40 (2013) 401–406. DOI: 10.1016/j.bios.2012.08.035

[52] D.-W. Zhang, F. Wu, J. Wang, M. Watkinson, S. Krause, Image detection of yeast *Saccharomyces cerevisiae* by light-addressable potentiometric sensors (LAPS), Electrochem. Commun. 72 (2016) 41–45. DOI: 10.1016/j.elecom.2016.08.017

[53] Y. Guo, C.F. Werner, A. Canales, L. Yu, X. Jia, P. Anikeeva, T. Yoshinobu, **Polymer-fiber-coupled field-effect sensors for label-free deep brain recordings**, PLoS ONE 15 (2020), art. no. e0228076. DOI: 10.1371/journal.pone.0228076

A miniature LAPS attached to the tip of an optical fiber bundle is inserted into the brain of a mouse as an imaging device. The implantable device records brain activity with the capability of electrophysiological imaging.

[54] Y. Guo, C. F. Werner, S. Handa, M. Wang, T. Ohshiro, H. Mushiake, T. Yoshinobu, Miniature multiplexed label-free pH probe in vivo, Biosens. Bioelectron. (2020) art. no. 112870. in press DOI: 10.1016/j.bios.2020.112870

[55] J. Wang, L. Du, S. Krause, C. Wu, P. Wang, **Surface modification and construction of LAPS towards biosensing applications**, Sens. Actuators, B 265 (2018) 161–173. DOI: 10.1016/j.snb.2018.02.190

A review of biosensing applications of LAPS as of 2018. A variety of sensor materials and surface modification technologies are summarized.

[56] W. Zhang, C. Liu, X. Zou, H. Zhang, X. Xu, Micrometer-scale light-addressable potentiometric sensor on an optical fiber for biological glucose determination, Anal. Chim. Acta 1123 (2020) 36–43. DOI: 10.1016/j.aca.2020.05.008

[57] C. Wu, A. Poghossian, T.S. Bronder, M.J. Schöning, Sensing of double-stranded DNA molecules by their intrinsic molecular charge using the light-addressable potentiometric sensor, Sens. Actuators B 229 (2016) 506–512. DOI: 10.1016/j.snb.2016.02.004

[58] Y. Tian, T. Liang, P. Zhu, Y. Chen, W. Chen, L. Du, C. Wu, P. Wang, Label-free detection of *E. Coli* O157:H7 DNA using light-addressable potentiometric sensors with highly oriented zno nanorod arrays, Sensors 19 (2019) art. no. 5473. DOI: 10.3390/s19245473

[59] Y. Jia, F. Li, T. Jia, Z. Wang, Meso-tetra(4-carboxyphenyl)porphine-enhanced DNA methylation sensing interface on a light-addressable potentiometric sensor, ACS Omega 4 (2019) 12567–12574. DOI: 10.1021/acsomega.9b00980

[60] Y. Jia, F. Li, **Studies of functional nucleic acids modified light addressable potentiometric sensors: X-ray photoelectron spectroscopy, biochemical assay, and simulation**, Anal. Chem. 90 (2018) 5153–5161. DOI: 10.1021/acs.analchem.7b05261

A LAPS surface was modified with functional nucleic acids (FNA) such as DNAzyme for Pb^{2+} sensing and aptamer for Ag^{+} sensing. LAPS measurements were assisted by XPS, biochemical assays and simulation (MEDICI).

[61] G. Li, W. Li, S. Li, X. Shi, J. Liang, J. Lai, Z. Zhou, A novel aptasensor based on light-addressable potentiometric sensor for the determination of Alpha-fetoprotein, Biochem. Eng. J. 164 (2020) art. no. 107780. DOI: 10.1016/j.bej.2020.107780

[62] W. Zhang, Y. Xu, H.E. Tahir, X. Zou, P. Wang, Rapid and wide-range determination of Cd(II), Pb(II), Cu(II) and Hg(II) in fish tissues using light addressable potentiometric sensor, Food Chem. 221 (2017) 541–547. DOI: 10.1016/j.foodchem.2016.11.141

[63] W. Zhang, Y. Xu, X. Zou, Rapid determination of cadmium in rice using an all-solid RGO-enhanced light addressable potentiometric sensor, Food Chem. 261 (2018) 1–7. DOI: 10.1016/j.foodchem.2018.04.022

Figure Captions

Figure 1. a) Typical setup of a LAPS. RE: reference electrode, CE: counter electrode, ϕ: potential difference at the electrolyte – insulator interface. b) Energy band diagrams explaining the generation of the transient currents in a LAPS after the light is turned on (left) and off (right). The electron – hole pairs generated by photoexcitation diffuse due to the concentration gradient toward the depletion layer, where they are separated by the internal field. c) Circuit model of a LAPS. I_{photo}: AC current source representing the transient currents generated in the depletion layer, I: LAPS signal current measured in the external circuit, C_{i}, C_{i}': capacitances of the insulator in the illuminated and non-illuminated areas, C_{d}, C_{d}': capacitances of the depletion layer in the illuminated and non-illuminated areas, Z: series resistance of the measurement circuit, Z_{lateral}: impedance of the solution in the lateral direction, Y: admittance representing the capacitive coupling of the solution and the semiconductor in the non-illuminated area. d) Current – voltage characteristics in the amplitude-mode LAPS (left) and SPIM (middle) and phase – voltage characteristics in the phase-mode LAPS (right).

Figure 2. a) Acidification rates related to the metabolism of three different kinds of bacteria (*E. coli*, *C. glutanicum*, *L. brevis*) in 1.67 mM glucose plotted as a function of cell numbers, simultaneously monitored on the same LAPS chip; reproduced from Ref. [38], open access publication under CC BY license. b) LAPS mechanism for extracellular recording of potential changes of cell membrane from taste receptor cells under bitter stimulation; reproduced from Ref. [50] with permission from Elsevier. c) AC photocurrent image of a mesenchymal stem cell on an InGaN surface (left) an optical image (right). In the color map, blue / red correspond to attached / non-attached cells; adapted from Ref. [14], open access publication under CC BY license. d) Photograph of miniature, all-in-one pH LAPS with its illustration of longitudinal sectional image (left) and example of real-time, *in vivo* multiplexed pH imaging (right) after 54 s toe-pinch stimulation of a rat (middle); adapted from Ref. [54] with permission from Elsevier.

Figure 3. a) Dynamic LAPS measurement for various glucose concentrations; reproduced from Ref. [56] with permission from Elsevier. b) Polymer degradation over time by the enzyme α-chymotrypsin utilizing ZnO nanorods for LAPS imaging; reproduced from Ref. [13] with permission from ACS publications. c) Shift of photocurrent-voltage curves of a LAPS with / without ZNO nanorods towards

single-stranded DNA in the nM concentration range; adpated from Ref. [58], open access publication under CC BY license. d) Calibration curve of a LAPS-based aptasensor for different AFP concentration; adapted from Ref. [61] with permission from Elsevier.

Table 1. Characteristics of LAPS for cell monitoring and biochemical sensing with category, target and technology (selected examples).

Category		Target	Technology	Reference
cell monitoring	quantification of cell metabolism (acidification)	*E. coli* (in orange juice)	LAPS (w. pH-sensitive hydrogel nanofiber)	[37]
		Corynebacterium glutamicum, *Lactobacillus brevis*,	LAPS	[38]
		E. coli	LAPS (w. paper fermentation broth)	[39]
		Corynebacterium glutamicum	LAPS	[40]
		breast cancer cell	LAPS (w. microfluidics)	[41]
			LAPS (w. pH-sensitive hydrogel nanofiber)	[42]
		hepatoma HepG2	LAPS (w. microfluidics)	[43,44]
		Chinese hamster ovary cell	LAPS (w. microfluidics and cryopreservation)	[45]
		macrophage	LAPS (w. magnetic beads loaded with endotoxin)	[46]
	detection and quantification of specific cell	circulating tumor cell	LAPS (w. antibody on carboxylated graphene oxide)	[47]
			LAPS (w. aptamer anchored on porous graphene oxide)	[48]
	monitoring of cell response to stimuli	adenosine triphosphate (ATP) from taste receptor cell	LAPS (w. ATP-sensitive aptamer)	[49]
		membrane potential change of and ATP release from taste receptor cell	LAPS (w. ATP-sensitive aptamer)	[50]
		extracellular potential of olfactory sensory neuron	LAPS	[51]
	imaging	*Saccharomyces cerevisiae*	LAPS	[52]
		human osteosarcoma cell, rat neuroblastoma cell	PEIS (photoelectrochemical imaging system)	[25]
		human osteosarcoma cell	AC photoelectrochemical imaging	[14]
		brain (mouse, rat)	LAPS (w. optical fiber bundle)	[53,54]
biosensing	enzyme-based biosensor	glucose in blood, urine	enzyme LAPS (w. optical fiber)	[56]
		enzymatic degradation of polymer	LAPS (w. ZnO nanorod)	[13]
	affinity-based biosensor	dsDNA	LAPS (w. positively charged PAH layer for electrostatic coupling)	[57]
		ssDNA of *E. coli* O157:H7 cell	LAPS (w. complimentary ssDNA for hybridization on ZnO nanorod)	[58]
		DNA methylation (5mC sites of ssDNA)	LAPS (w. target ssDNA anchored on sensor and 5mC-antibody added)	[59]
		Pb^{2+}, Ag^{+}	functional nucleic acid (FNA)-LAPS (w. DNAzyme for Pb^{2+}, aptamer for Ag^{+})	[60]
		Alpha-fetoprotein	LAPS (w. aptamer)	[61]
application to food analysis		Cd^{2+}, Pb^{2+}, Cu^{2+}, Hg^{2+} in fish	LAPS (w. ionophore)	[62]
		Cd^{2+} in rice	LAPS (w. ionophore on reduced graphene oxide)	[63]

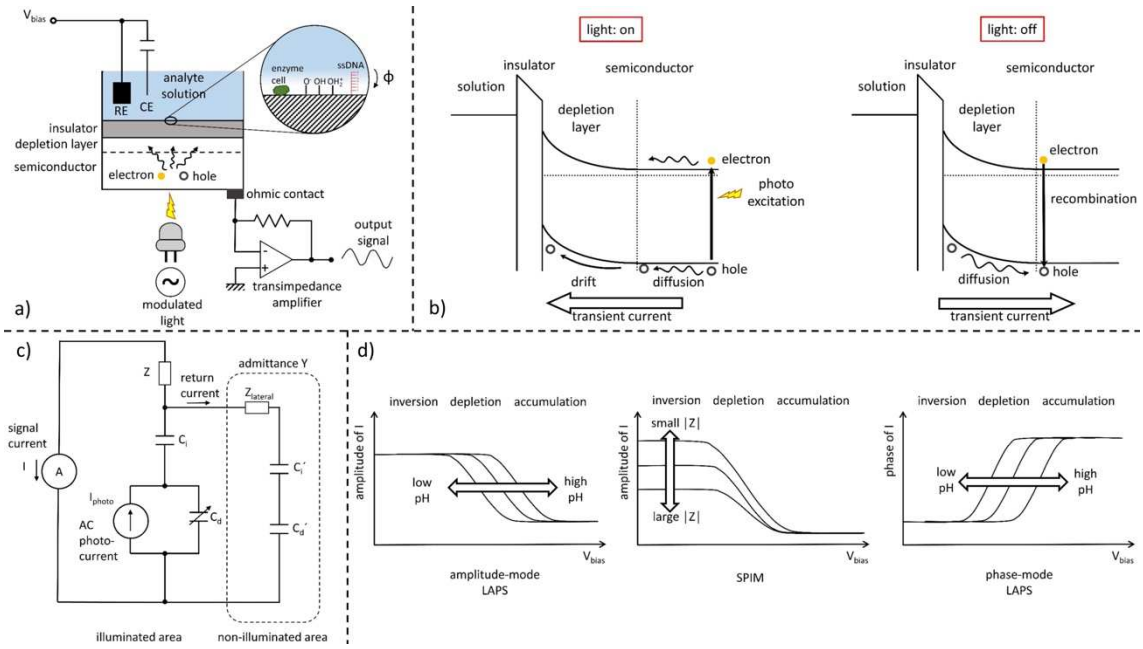

Figure 1. a) Typical setup of a LAPS. RE: reference electrode, CE: counter electrode, ϕ: potential difference at the electrolyte – insulator interface. b) Energy band diagrams explaining the generation of the transient currents in a LAPS after the light is turned on (left) and off (right). The electron – hole pairs generated by photoexcitation diffuse due to the concentration gradient toward the depletion layer, where they are separated by the internal field. c) Circuit model of a LAPS. I_{photo}: AC current source representing the transient currents generated in the depletion layer, I: LAPS signal current measured in the external circuit, C_{i}, C_{i}': capacitances of the insulator in the illuminated and non-illuminated areas, C_{d}, C_{d}': capacitances of the depletion layer in the illuminated and non-illuminated areas, Z: series resistance of the measurement circuit, Z_{lateral}: impedance of the solution in the lateral direction, Y: admittance representing the capacitive coupling of the solution and the semiconductor in the non-illuminated area. d) Current – voltage characteristics in the amplitude-mode LAPS (left) and SPIM (middle) and phase – voltage characteristics in the phase-mode LAPS (right).

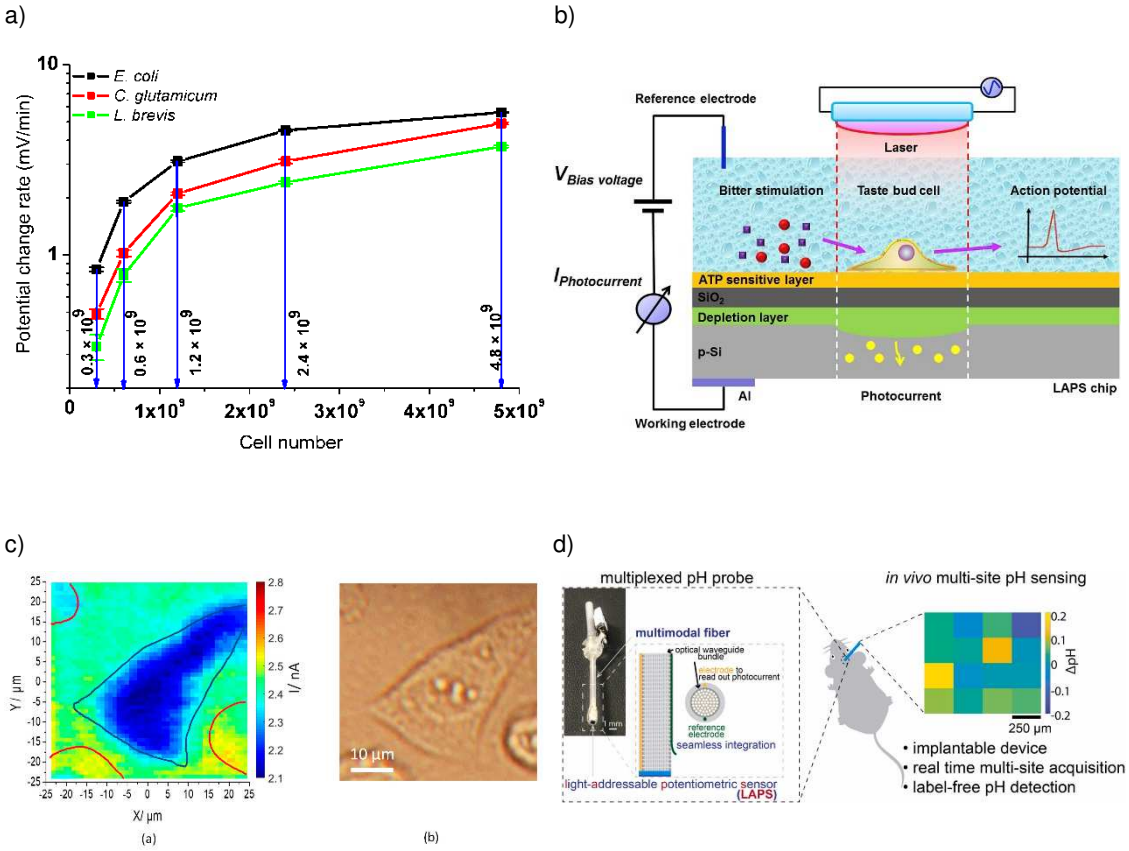

Figure 2. a) Acidification rates related to the metabolism of three different kinds of bacteria (*E. coli*, *C. glutanicum*, *L. brevis*) in 1.67 mM glucose plotted as a function of cell numbers, simultaneously monitored on the same LAPS chip; reproduced from Ref. [38], open access publication under CC BY license. b) LAPS mechanism for extracellular recording of potential changes of cell membrane from taste receptor cells under bitter stimulation; reproduced from Ref. [50] with permission from Elsevier. c) AC photocurrent image of a mesenchymal stem cell on an InGaN surface (left) an optical image (right). In the color map, blue / red correspond to attached / non-attached cells; adapted from Ref. [14], open access publication under CC BY license. d) Photograph of miniature, all-in-one pH LAPS with its illustration of longitudinal sectional image (left) and example of real-time, *in vivo* multiplexed pH imaging (right) after 54 s toe-pinch stimulation of a rat (middle); adapted from Ref. [54] with permission from Elsevier.

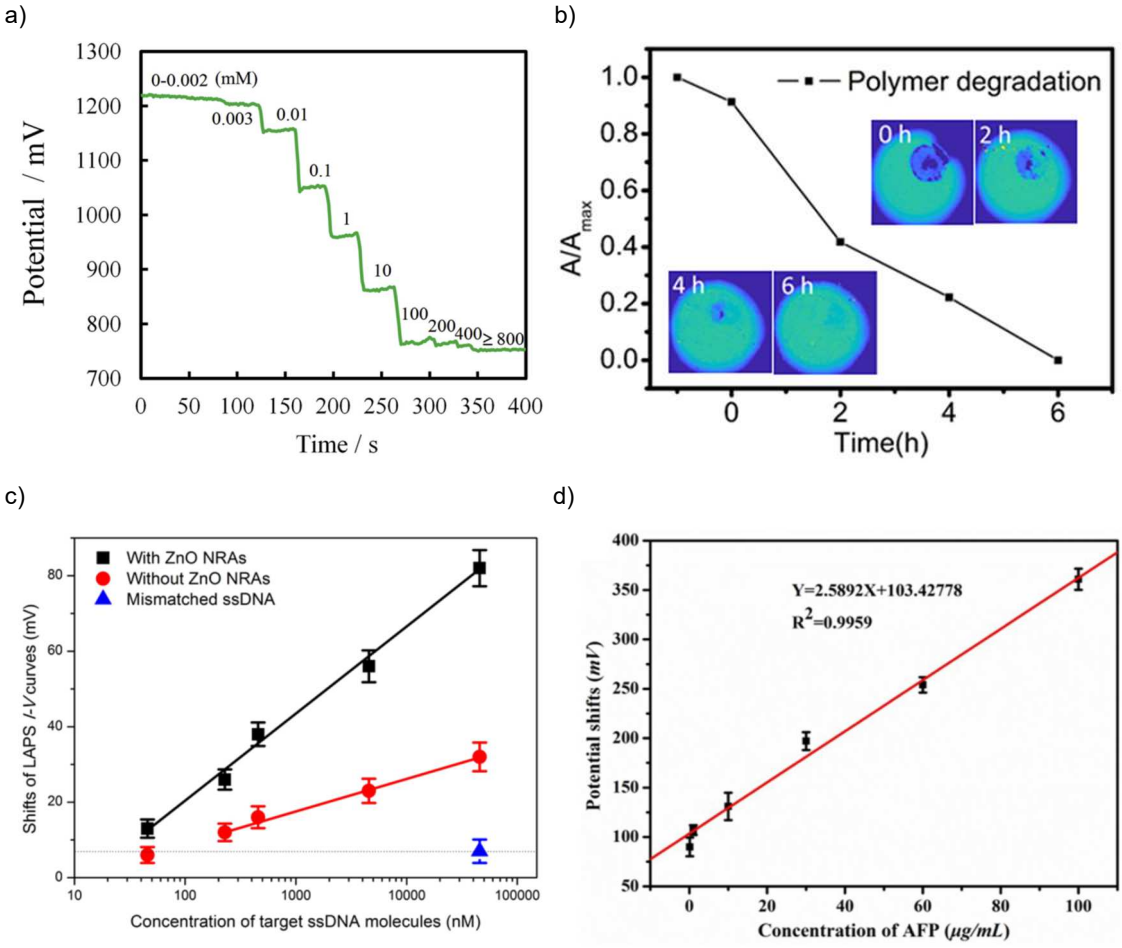

Figure 3. a) Dynamic LAPS measurement for various glucose concentrations; reproduced from Ref. [56] with permission from Elsevier. b) Polymer degradation over time by the enzyme α-chymotrypsin utilizing ZnO nanorods for LAPS imaging; reproduced from Ref. [13] with permission from ACS publications. c) Shift of photocurrent-voltage curves of a LAPS with / without ZNO nanorods towards single-stranded DNA in the nM concentration range; adpated from Ref. [58], open access publication under CC BY license. d) Calibration curve of a LAPS-based aptasensor for different AFP concentration; adapted from Ref. [61] with permission from Elsevier.

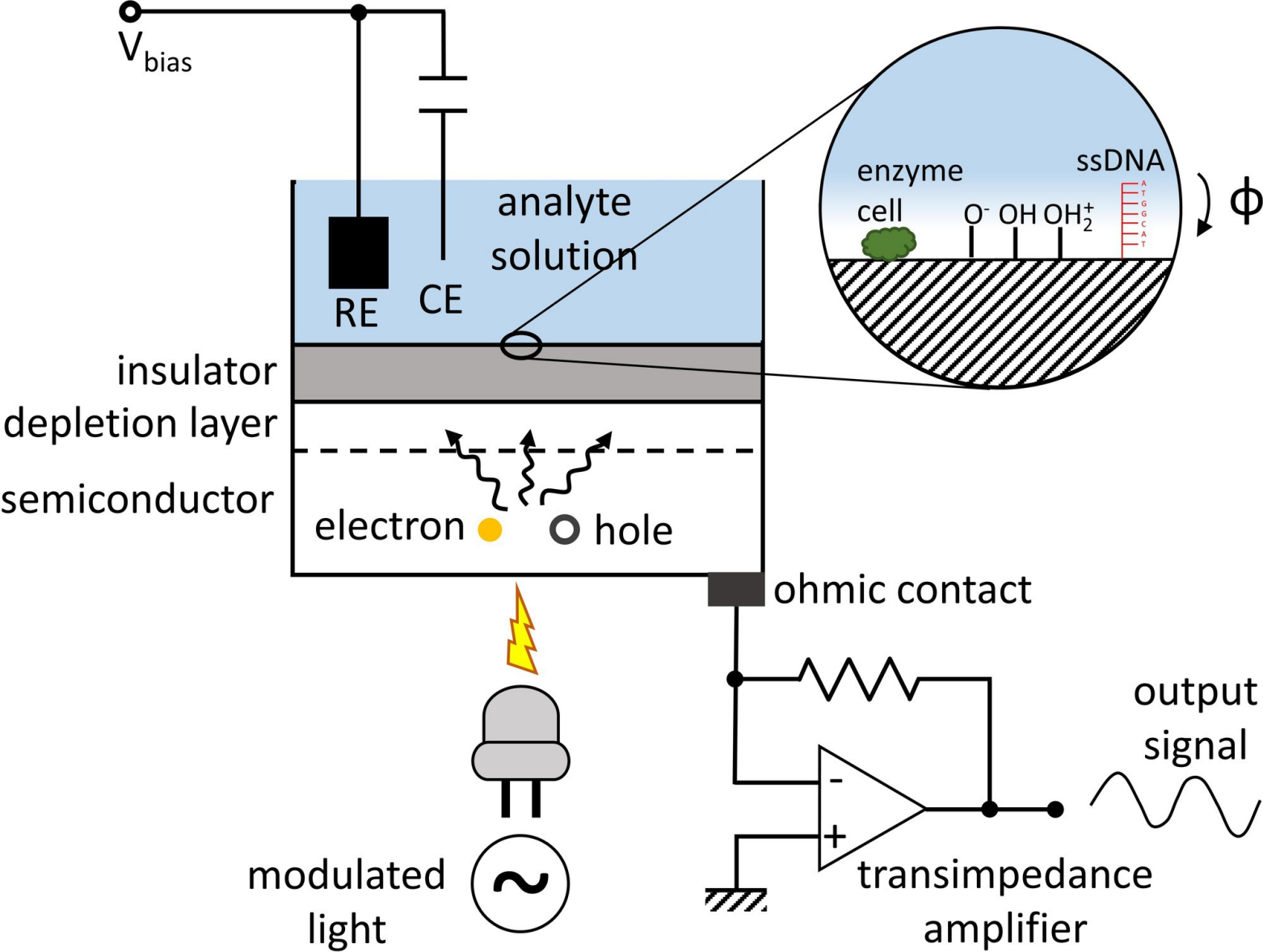
V bias
RE
CE
analyte solution
insulator
depletion layer
semiconductor
electron
hole
enzyme cell
ssDNA
O- OH OH2+
ϕ
ohmic contact
output signal
modulated light
transimpedance amplifier